Magnetic properties of a novel quasi-2D Cu(II)-trimer system



2009 J. Phys.: Condens. Matter 21 185013

(http://iopscience.iop.org/0953-8984/21/18/185013)

J. Phys.: Condens. Matter **21** (2009) 185013 (7pp) doi:10.1088/0953-8984/21/18/185013

# Magnetic properties of a novel quasi-2D Cu(II)-trimer system

**Katarina Remović-Langer[1], Eiken Haussühl[2], Leonore Wiehl[2], Bernd Wolf[1], Francesca Sauli[3], Nils Hasselmann[4], Peter Kopietz[3] and Michael Lang[1]**

[1] Physikalisches Institut, Universität Frankfurt, SFB/TRR-49, D-60438 Frankfurt, Germany
[2] Institut für Geowissenschaften, Universität Frankfurt, D-60438 Frankfurt, Germany
[3] Institut für Theoretische Physik, Universität Frankfurt, SFB/TTR-49, D-60438 Frankfurt, Germany
[4] International Center of Condensed Matter Physics, Universidade de Brasília, 70910-900 Brasília, Brazil

Received 13 October 2008, in final form 17 February 2009
Published 6 April 2009
Online at stacks.iop.org/JPhysCM/21/185013

**Abstract**

We present structural and magnetic data of a new $Cu^{2+}(S = 1/2)$-containing magnetic trimer system $2b{\cdot}3CuCl_2{\cdot}2H_2O$ (b = betaine, $C_5H_{11}NO_2$). The trimers form a quasi-2D quantum spin system with an unusual *intra*-layer exchange coupling topology, which, in principle, supports diagonal four-spin exchange. To describe the magnetic properties, a 2D effective interacting-trimer model has been developed including an *intra*-trimer coupling $J$ and two *inter*-trimer couplings $J_a$ and $J_b$. The low-energy description and effective parameters are obtained from numerical calculations based on four coupled trimers (with periodic boundary conditions). Fits to the experimental data using this model yield the magnetic coupling constants $J/k_B = -15$ K and $J_a/k_B = J_b/k_B = -4$ K. These parameters describe the susceptibility and magnetization data very well over the whole temperature and field range investigated. Moreover, the model calculations indicate that, for certain ranges of the ratio $J_b/J_a$, which might be accessible by either chemical substitution and/or hydrostatic pressure, the low-energy properties of $2b{\cdot}3CuCl_2{\cdot}2H_2O$ will be dominated by non-trivial four-spin exchange processes.

(Some figures in this article are in colour only in the electronic version)

## 1. Introduction

Quantum magnetism in reduced dimensions is of great interest in solid state physics due to the wealth of exciting phenomena originating from the interplay of reduced dimensionality (reduced D), competing interactions and strong quantum fluctuations. Low-D quantum magnets now offer exciting possibilities for testing fundamental concepts of theoretical physics, where formally they were only considered to be of academic interest [1, 2]. Therefore, also in material science, many activities have been directed towards a rational design of low-D quantum spin systems with novel exchange coupling topologies [3, 4]. Metal–organic Cu(II) compounds especially, where one finds a large variety of suitable bridging ligands, are used to realize various kinds of magnetic topologies such as coupled spin-dimer systems, spin chains or magnetic trimer systems.

An important family of magnetic trimer systems, which has been intensively investigated in the past, is provided by the copper halide salts [5, 6 and references therein]. In this group of materials, the individual trimers are coupled into stacks, thereby forming quasi-1D spin structures. Their unusual magnetic properties have been described by a high-temperature series expansion for the Heisenberg model with the *inter*-trimer coupling constants as expansion parameters [7]. Due to their quasi-1D character, the copper halide salts have also served as model systems for ferromagnetically coupled Heisenberg chains. Besides their use for addressing fundamental aspects of quantum magnetism, magnetic trimer systems have attracted considerable interest also for technical applications such as catalysts, molecular sieves and ion exchangers, see, e.g., [8, 9].

Here we present a new magnetic Cu(II)-trimer system $2b{\cdot}3CuCl_2{\cdot}2H_2O$ (b = betaine, $C_5H_{11}NO_2$), where the trimers form a quasi-2D quantum spin system with an unusual

 

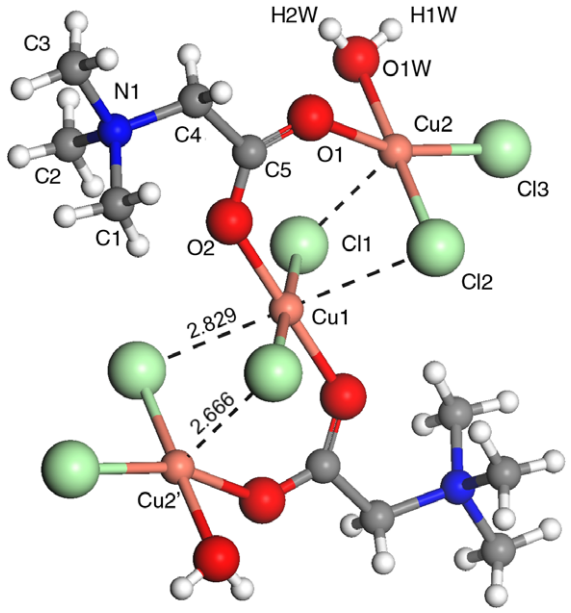


**Figure 1.** Trinuclear copper complexes bridged by the carboxylate groups O1–C5–O2 of two betaine molecules. Broken lines indicate the semi-coordination between copper and chlorine ions with $d(\mathrm{Cu1}\cdots\mathrm{Cl2}) = 2.829$ Å and $d(\mathrm{Cu2}\cdots\mathrm{Cl1}) = 2.666$ Å.

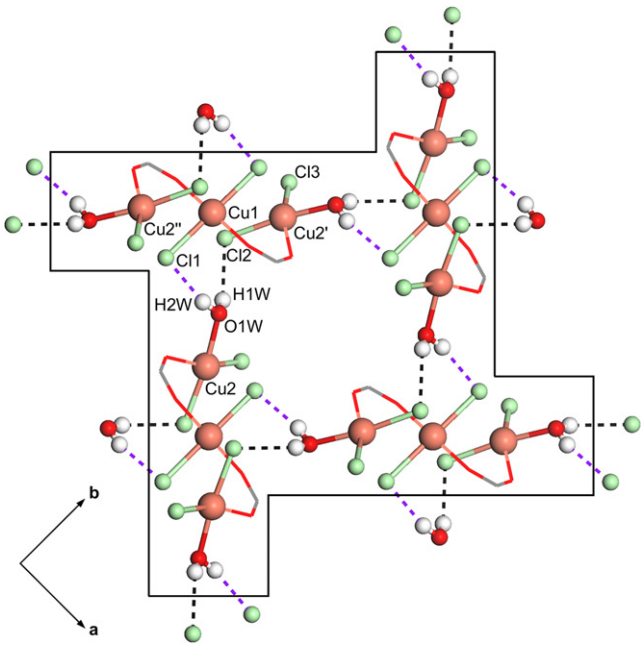


**Figure 2.** Projection approximately along the $c$ axis of one layer of a plaquette of four hydrogen-bonded trimers; cf the effective interacting-trimer model shown in figure 6. Copper and chlorine ions and water molecules are shown as spheres. The carboxylate bridges are indicated by lines and the rest of the betaine molecules have been omitted for clarity. Dashed lines indicate hydrogen bonds.

intra-layer exchange coupling topology, which in principle supports ring-exchange processes. Only a few examples of 2D coupled-trimer systems are known up to now, see, e.g., [10]. We discuss structural aspects together with magnetic susceptibility and magnetization data of this compound and present a theoretical model which enables us to describe the magnetic properties over a wide temperature and field range.

## 2. Experimental details

Green plate-like crystals of $2\mathrm{b}{\cdot}3\mathrm{CuCl_2}{\cdot}2\mathrm{H_2O}$ were grown from an aqueous solution of betaine monohydrate ($\mathrm{C_5H_{11}NO_2}{\cdot}\mathrm{H_2O}$) and copper dichloride dihydrate ($\mathrm{CuCl_2}{\cdot}2\mathrm{H_2O}$) with a molar ratio of 2:3 by slow evaporation of the solvent at ambient temperature. The crystal structure was determined by x-ray diffraction with Mo K$\alpha$ radiation, using a four-circle diffractometer Xcalibur3 from Oxford Diffraction equipped with a CCD camera [11].

The magnetic susceptibility and isothermal magnetization of $2\mathrm{b}{\cdot}3\mathrm{CuCl_2}{\cdot}2\mathrm{H_2O}$ were measured in the temperature range $2\ \mathrm{K} \leqslant T \leqslant 300\ \mathrm{K}$ and in magnetic fields $B \leqslant 5$ T using a Quantum Design SQUID magnetometer. All data have been corrected for the temperature-independent diamagnetic core contribution according to [4]. The measurements were performed on a large single crystal with a mass of $m = 46.29$ mg randomly oriented with respect to the external field.

## 3. Structural aspects

The compound $2\mathrm{b}{\cdot}3\mathrm{CuCl_2}{\cdot}2\mathrm{H_2O}$ crystallizes in the space group $Pbca$, with lattice parameters $a = 11.1814(1)$ Å, $b = 11.438\,30(10)$ Å, $c = 18.8671(2)$ Å and $\alpha = \beta = \gamma = 90°$. The crystal structure consists of neutral, trinuclear copper complexes, which are located at inversion centers. As shown in figure 1, inside each trimer the copper ions are linked pairwise by the carboxylate groups of the betaine molecules. Each of the $Cu^{2+}$ ions exhibits a nearly planar quadratic coordination by two oxygen and two chlorine atoms, indicating that the unpaired electron is located in the $d_{x^2-y^2}$ orbital. In addition, a semi-coordination between the magnetic centers exists within each dimer via the chlorine atoms (broken lines in figure 1). As a consequence, the central Cu1 ion has a $4+2$ coordination, whereas the terminal Cu2 ions exhibit only a $4+1$ coordination. With $d(\mathrm{Cu1}\cdots\mathrm{Cl2}) = 2.829$ Å and $d(\mathrm{Cu2}\cdots\mathrm{Cl1}) = 2.666$ Å these bond lengths are similar to the ones found in various copper trimer systems exhibiting semi-coordinated $Cu^{2+}$ ions [5, 6].

As displayed in figure 2, the trimers are interconnected in the (001) plane via a network of O–H$\cdots$Cl hydrogen bonds. These layers of Cu trimers are stacked along the $c$ axis with a translation period of two layers related by mirror symmetry. The layers are connected by weak van der Waals bonds along the $c$ axis. Figure 2 shows the arrangement of four hydrogen-bonded trimers within one layer. There are two different hydrogen bridges involved connecting the individual trimers, namely the path Cu2–O1W–H2W$\cdots$Cl1–Cu1 with a total length of 7.439 Å (direct Cu2–Cu1 distance $d(\mathrm{Cu2–Cu1}) = 5.667$ Å, $d(\mathrm{H2W}\cdots\mathrm{Cl1}) = 2.320$ Å) and the path Cu2–O1W–H1W$\cdots$Cl2–Cu2′ with a total length of 7.441 Å ($d(\mathrm{Cu2–Cu2'}) > 6$ Å, $d(\mathrm{H1W}\cdots\mathrm{Cl2}) = 2.400$ Å).

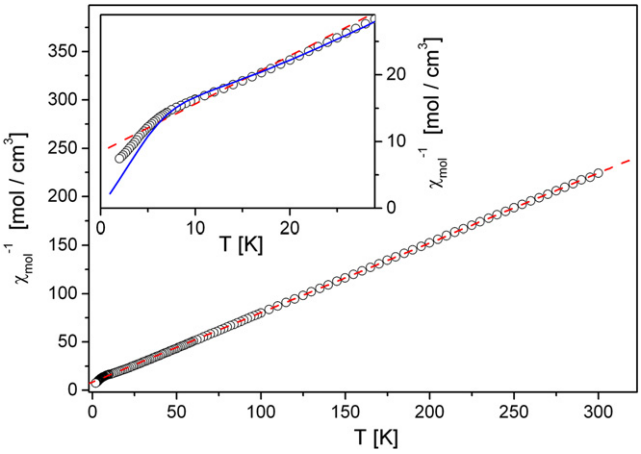


**Figure 3.** The inverse molar magnetic susceptibility of $2b{\cdot}3CuCl_2{\cdot}2H_2O$ in the temperature range 2–300 K. Data were taken at a magnetic field of 0.05 T. The dashed line is a Curie–Weiss fit in the temperature range 100 K $\leqslant T \leqslant$ 300 K. Inset: low-temperature data of $\chi_{mol^{-1}}(T)$ together with the Curie–Weiss fit (dashed line) obtained at high temperatures and a fit based on a theoretical model [13] for isolated non-interacting trimers (solid line).

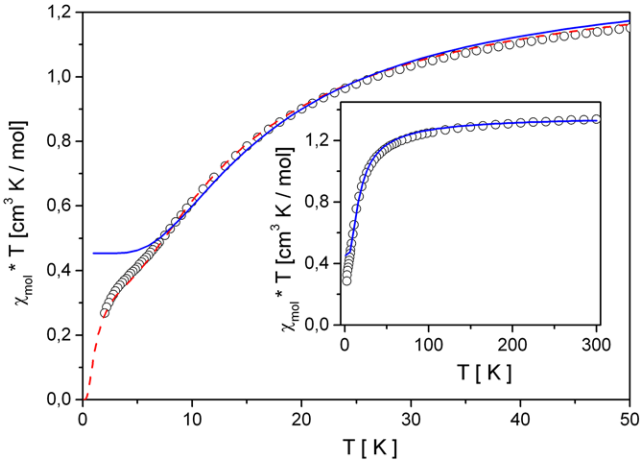


**Figure 4.** Main panel: magnetic susceptibility of $2b{\cdot}3CuCl_2{\cdot}2H_2O$ from 2 to 50 K taken at a field of 0.05 T plotted as $\chi_{mol}T$ versus $T$. The solid line represents a fit to the experimental data using an isolated-trimer model with an *intra*-trimer coupling constant of $J/k_B = -20$ K. The dashed line corresponds to the best fit of the 2D coupled-trimer model (based on an exact diagonalization of four coupled trimers) with $J/k_B = -15$ K and $J_a/k_B = J_b/k_B = -4$ K. See the text for details. Inset: magnetic susceptibility as $\chi_{mol}T$ over the whole temperature range investigated together with a fit using the isolated-trimer model (solid line).

## 4. Magnetic properties

Figure 3 shows the molar magnetic susceptibility $\chi_{mol}(T) = M(T)/B$ of $2b{\cdot}3CuCl_2{\cdot}2H_2O$ in a representation $\chi_{mol}^{-1}(T)$ versus $T$, where $M$ denotes the magnetic moment of the sample. The data are taken at a small field of $B = 0.05$ T. The magnetic moment $M$ is reversible upon cooling and heating with no indication of hysteretic behavior. In addition, no signature of a long-range magnetic order can be observed down to 2 K, the lowest temperature of our experiment.

The figure discloses, to a good approximation, two almost linear regimes of $\chi_{mol}^{-1}(T)$ that are separated by a crossover range. For temperatures 100 K $\leqslant T \leqslant$ 300 K $\chi_{mol}$ follows a Curie–Weiss-like temperature dependence $\chi_{mol} = C_m/(T - \Theta_{CW})$. A least-squares fit in this temperature range (dashed curve in figure 3) yields a molar Curie constant $C_m = 1.390$ cm$^3$ K mol$^{-1}$, corresponding to three $Cu^{2+}$ ions per formula unit, and a Weiss temperature $\Theta_W = -11.8$ K. Analyzing the $\chi_{mol}T$ data at 300 K one obtains at this temperature an effective magnetic moment per $Cu^{2+}$ ion of $\mu_{eff} = 1.892\mu_B$ and a molar Curie constant $C_m = 1.339$ cm$^3$ K mol$^{-1}$. Both numbers are based on an average $g$ factor of 2.185. The effective magnetic moment and the $g$ value at 300 K are consistent with the local Cu coordination of $2b{\cdot}3CuCl_2{\cdot}2H_2O$. The negative Weiss temperature implies that the magnetic interactions between the $Cu^{2+}$ ions have a predominantly antiferromagnetic character. From the approximately linear temperature dependence of $\chi_{mol}^{-1}(T)$ below 5 K (see the inset of figure 3), yielding a distinctly larger slope compared to the high-temperature regime, a reduced magnetic moment at low temperatures can be inferred. The inset of figure 3 gives an expanded view of the low-temperature $\chi_{mol}^{-1}(T)$ data. For comparison, we show the Curie–Weiss behavior (dashed line) obtained by fitting the high-temperature data, as well as the result of a least-squares fit (solid line) to a model of isolated non-interacting trimers [13]. While the latter model provides a reasonable description of $\chi_{mol}^{-1}(T)$ at high temperatures, see the discussion below, it markedly deviates from the data below about 5 K. These deviations indicate that—as expected from the crystal structure—the ground state of the system is more complex and additional interactions have to be invoked to properly describe the coupled 2D-trimer system at low temperatures.

The magnetic susceptibility of $2b{\cdot}3CuCl_2{\cdot}2H_2O$, which is reminiscent of that observed in a variety of magnetic trimer systems [5, 13, 6, 12 and references therein], suggests that the magnetic behavior is dominated by an antiferromagnetic *intra*-trimer exchange interaction $J$. In a first approach, which has been applied also to other trimer systems [13], we therefore consider isolated linear $Cu^{2+}(S = 1/2)$ trimers with two equivalent magnetic *intra*-trimer exchange interactions $J$ mediated via the carboxylate groups and the semi-coordinated chlorine atoms, cf figure 1. The corresponding spin Hamiltonian is given by

$$\hat{H} = -J(\hat{S}_1\hat{S}_2 + \hat{S}_2\hat{S}_3) - g\mu_B\vec{B}(\hat{S}_1 + \hat{S}_2 + \hat{S}_3). \quad (1)$$

In [13] an expression for the magnetic susceptibility of equation (1) has been derived. By fitting equation (2) of [13] to the susceptibility data at $T \geqslant 6$ K the dominant antiferromagnetic *intra*-trimer exchange coupling constant can be derived.

The best fit for isolated trimers is shown again in figure 4 (solid line), where the susceptibility is plotted as $\chi_{mol}T$ versus $T$. In this representation, the temperature dependence of the magnetic moment, especially at low temperatures, can be visualized more clearly. The $\chi_{mol}T$ data are only weakly temperature-dependent down to 100 K, cf the inset of figure 4,

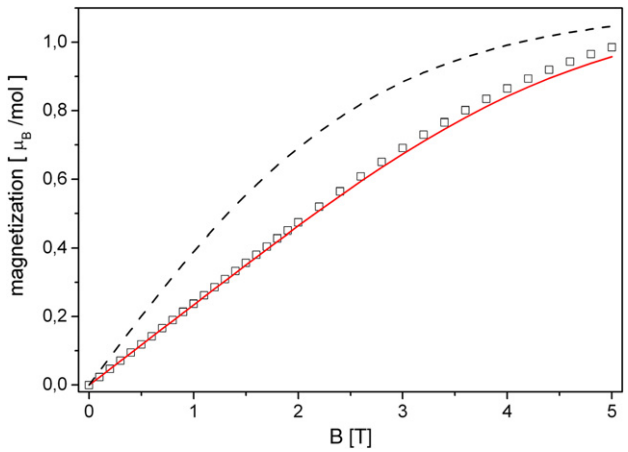


**Figure 5.** Isothermal magnetization measurements at $T = 2$ K in dc fields up to 5 T with the coupling parameters given in the text. Broken line: magnetization of an independent trimer at $T = 2$ K. The solid line shows the result of an exact diagonalization of the coupled-trimer model.

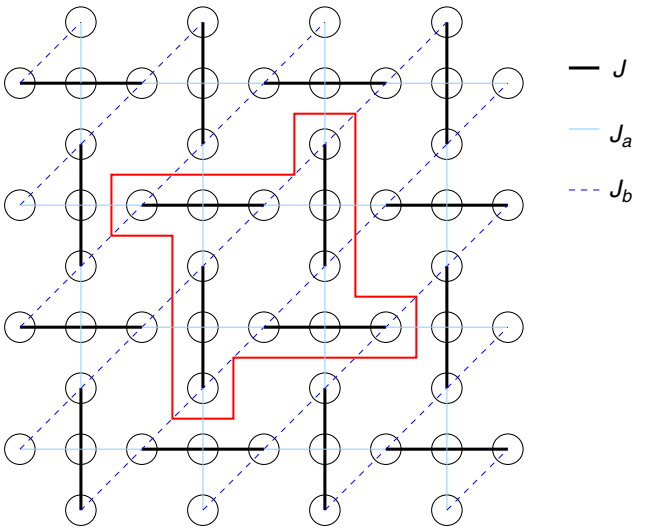


**Figure 6.** Effective interacting-trimer model with *intra*-trimer coupling $J$ and two types of *inter*-trimer coupling $J_a$, $J_b$. The central region was used in the numerical calculations and contains four coupled trimers (with periodic boundary conditions).

below which the magnetic moment becomes strongly reduced. Figure 4 indicates that a reasonable description of the data down to 6 K is achieved by the independent-trimer model with a moderate coupling constant $J/k_B = -20$ K. At low temperatures (the main panel of figure 4), however, the model curve starts to deviate quite considerably from the data, indicating the presence of additional, weaker *inter*-trimer interactions.

A significant improvement of the model curve can be achieved by the incorporation of *inter*-trimer couplings. An effective interacting-trimer model, the energy spectrum for variable *inter*-trimer couplings and expressions for the resulting magnetic properties will be discussed in the subsequent section. For application to the present material, and in order to reduce the number of adjustable parameters to a minimum, we set the two *inter*-trimer coupling constants $J_a = J_b$. This appears justified given the nearly similar Cu–O–H$\cdots$Cl–Cu path lengths. The dashed curve in the main panel of figure 4 shows the resulting best fit obtained by fitting the data over the whole temperature range investigated. As the figure clearly demonstrates, the model of 2D coupled trimers with $J/k_B = -15$ K and $J_a/k_B = J_b/k_B = -4$ K describes the susceptibility data very well (the calculation is based on an exact diagonalization of the four-trimer cluster shown in figure 6). The small difference between the experimental data and the fit for temperatures below 6 K, corresponding to an offset in $\chi_{mol}T$ of approximately 0.014 cm$^3$ K mol$^{-1}$, is likely due to a small amount of paramagnetic impurities. The latter may result from uncoupled $Cu^{2+}$ ions for which $\chi_{mol}T = 0.014$ cm$^3$ K mol$^{-1}$ would correspond to a concentration of $(4 \pm 1)\%$, a reasonable value for a single crystal grown from an aqueous solution.

Further support for the applicability of the above 2D coupled-trimer model can be gained from the results of the isothermal magnetization in figure 5. The figure shows the experimental data, taken at 2 K, together with the magnetization calculated for the 2D coupled-trimer system (solid line) and the independent trimers (broken line), using the same coupling constants as derived from the corresponding fits to the susceptibility data. While significant deviations become evident for the independent-trimer model, the 2D coupled-trimer model provides a very good description of the $M(B, T = 2\text{ K})$ data.

## 5. Low-energy description: effective parameters

At very low temperatures $k_BT \ll J_a, J_b$ correlations beyond the finite-sized cluster that we used in the exact diagonalization study will become important. Since the original trimer structure is rather complex, a detailed study of the very low-energy structure and the study of possible ordered states requires the development of a simpler effective low-energy model which captures the dominant interaction among the trimers. Although we will not present here a complete analysis of the low-energy effective model, nonetheless we want to derive the dominant coupling parameters which emerge at low energies from the model.

As discussed above, from the crystal structure of $2b{\cdot}3CuCl_2{\cdot}2H_2O$ one would expect that, to a good approximation, both *inter*-trimer exchange parameters $J_a$ and $J_b$ to be equal—an assumption which is also corroborated by the success in describing the experimental data. For completeness, we shall treat in this section the more general case and allow $J_a$ and $J_b$ to vary independently.

At low temperatures $k_BT \ll J$ the trimers are mostly in their ground state [13]. Since the trimer ground state has $S = 1/2$, the system can, for low temperatures, be described by a reduced low-energy model of coupled $S = 1/2$ spins—one for each trimer—and the trimer model considered here reduces then to a square lattice of $S = 1/2$ spins. What are the interactions between these effective spins? If the *inter*-trimer interactions $J_a$, $J_b$ are much smaller than the *intra*-trimer

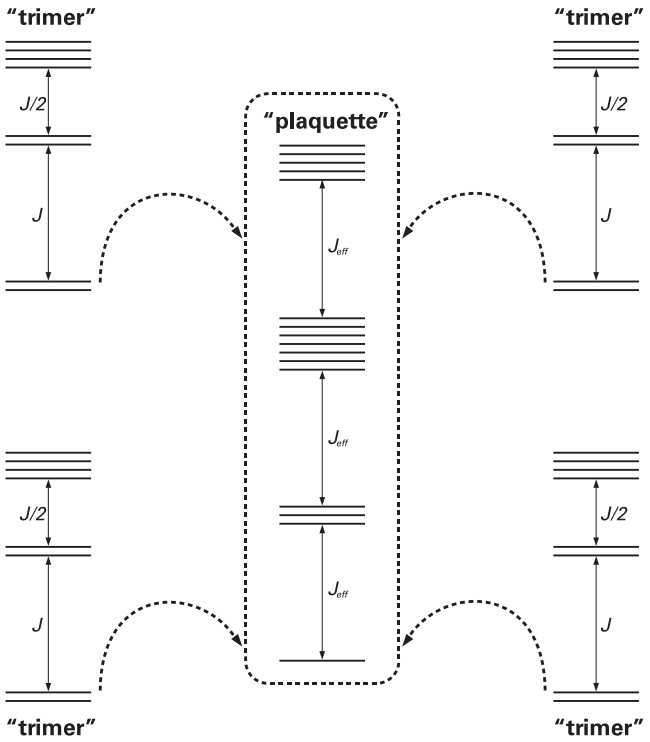


**Figure 7.** The *intra*-trimer coupling yields at low energies an effective theory of coupled $S = 1/2$ states. Assuming an antiferromagnetic exchange $J_{\rm eff} > 0$, leading-order perturbation theory predicts that the ground state of the plaquette is a singlet and the lowest excited states are an $S = 1$ triplet separated by $J_{\rm eff}$ from the ground state (assuming here $J_{\rm eff} > 0$). Again at an energy $J_{\rm eff}$ higher are two degenerate $S = 1$ triplets and an $S = 0$ singlet. The highest-energy state with all trimers still in their ground state is the $S = 2$ ferromagnetic state.

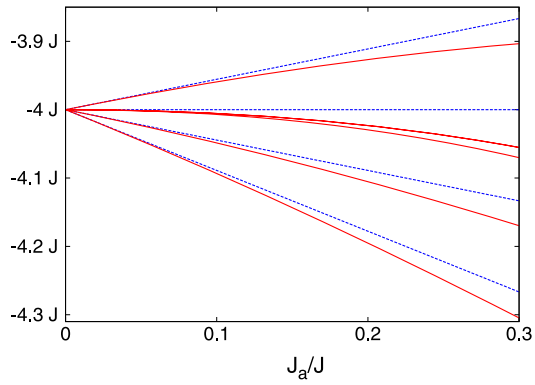


**Figure 8.** Evolution of the lowest eigenenergies of the full 12-spin cluster (obtained from exact diagonalization) as a function of the *inter*-trimer coupling $J_{\rm a} = J_{\rm b}$. These lowest-energy levels all originate from states where each trimer is in its $S = 1/2$ ground state. Also shown (dashed lines) is the result of lowest-order perturbation theory which yields an effective nearest-neighbor coupling of the spins with $J_{\rm eff} = (4/9)(J_{\rm b} - J_{\rm a}/2)$. The deviation of the full calculation from lowest-order perturbation theory can be accounted for by the inclusion of four-spin exchange processes and next-to-nearest-neighbor interactions which are of higher order in $J_{\rm a/b}/J$.

interaction $J$, one can use perturbation theory to calculate effective exchange parameters for the reduced model. First-order perturbation theory reveals that the dominant effective exchange interaction of the $S = 1/2$ trimer states is a nearest-neighbor coupling of strength $J_{\rm eff} = (4/9)(J_{\rm b} - J_{\rm a}/2)$. This implies that even if all bare spin interactions are antiferromagnetic, the effective nearest-neighbor interaction among the trimers becomes ferromagnetic if $J_{\rm b} < J_{\rm a}/2$. A similar dependence of the effective coupling of the bare *inter*-trimer exchange parameters was reported for trimer chains [7]. The low-energy states which result from the leading-order perturbation theory of the 12-spin model forming a plaquette of trimers is shown schematically in figure 7. In the corners are also shown the energy levels of each trimer which consist of an $S = 1/2$ ground state, an $S = 1/2$ excited state and an $S = 3/2$ state at energy $3J/2$ above the ground state. For illustration we plotted in figure 8 the evolution of the lowest exact eigenenergies of the 12-spin cluster as a function of the *inter*-trimer interaction (as an example we pick here again $J_{\rm a} = J_{\rm b}$). All five visible eigenenergies can be identified with those of a reduced plaquette model, where each of the four trimers is in its $S = 1/2$ ground state. Also shown is the prediction of first-order perturbation theory. For intermediate values of $J_{\rm a}$, one clearly observes in figure 8 deviations from first-order perturbation theory. At even larger values, near $J_{\rm a}/J = 0.4$, new states, which emerge from excited trimer states, start to mix with the $S = 1/2$ ground states of the trimers. For such large values it is no longer possible to describe the trimers in terms of effective $S = 1/2$ states only and we will therefore not pursue this regime.

The deviations of the low-energy levels from first-order perturbation theory, seen in figure 8, can be accounted for in the reduced model if additional effective exchange parameters, besides the simplest nearest-neighbor exchange, are included. Since higher-order perturbation theory quickly becomes cumbersome, we calculate instead the effective parameters numerically and project from the full trimer model onto the reduced model where each trimer is represented by only one spin with $S = 1/2$. For one plaquette, this can be done exactly. Let us first investigate the most general $S = 1/2$ Hamiltonian on a four-spin plaquette. It can be written as $\hat{H} = \hat{H}_1 + \hat{H}_2 + \hat{H}_3 + \hat{H}_4$ [14], with

$$\hat{H}_1 = j_1(\hat{S}_1 \cdot \hat{S}_2 + \hat{S}_2 \cdot \hat{S}_3 + \hat{S}_3 \cdot \hat{S}_4 + \hat{S}_4 \cdot \hat{S}_1),$$
$$\hat{H}_2 = j_2(\hat{S}_1 \cdot \hat{S}_3 + \hat{S}_2 \cdot \hat{S}_4),$$
$$\hat{H}_3 = j_3((\hat{S}_1 \cdot \hat{S}_2)(\hat{S}_3 \cdot \hat{S}_4) + (\hat{S}_1 \cdot \hat{S}_4)(\hat{S}_2 \cdot \hat{S}_3) - (\hat{S}_1 \cdot \hat{S}_3)(\hat{S}_2 \cdot \hat{S}_4)),$$
$$\hat{H}_4 = j_4(\hat{S}_1 \cdot \hat{S}_3)(\hat{S}_2 \cdot \hat{S}_4).$$

The first part, $\hat{H}_1$, is just the usual nearest-neighbor exchange. This term was already predicted by perturbation theory. The other terms are $\hat{H}_2$, which describes next-to-nearest-neighbor exchange, $\hat{H}_3$, which arises from a four-spin cyclic exchange, and $H_4$, which describes a four-spin exchange via the diagonals of the plaquette. The energy spectrum of this model can be calculated analytically. It consists of two singlet states with energies $E_{S=0,\rm a} = -2j_1 + (1/2)j_2 + (13/16)j_3 + (1/16)j_4$ and $E_{S=0,\rm b} = -(3/2)j_2 - (3/16)j_3 + (9/16)j_4$ (we use the subscripts a and b to differentiate between states with the same total spin quantum number), two degenerate triplet states with energy $E_{S=1,\rm a} = -(1/2)j_2 + (1/16)j_3 - (3/16)j_4$, a

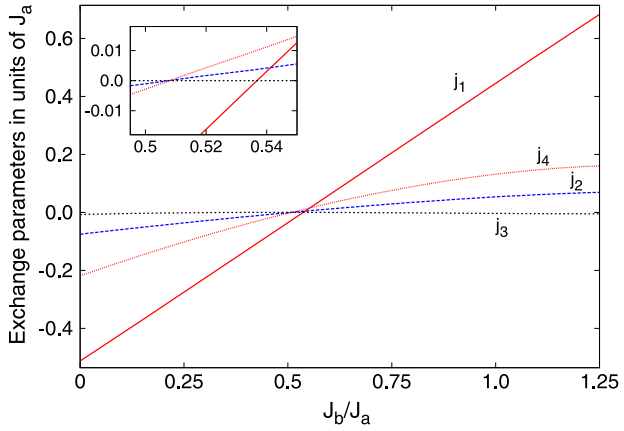


**Figure 9.** Effective low-energy exchange parameters plotted as a function of the bare ones, calculated with exact diagonalization (see the text). The parameters of the bare ones are $J_a/J = 0.2$ and $J_b/J_a$ varies as shown in the label.

further triplet state with energy $E_{S=1,b} = -j_1 + (1/2)j_2 - (7/16)j_3 + (1/16)j_4$ and finally a $S = 2$ state with energy $E_{S=2} = j_1 + (1/2)j_2 + (1/16)j_3 + (1/16)j_4$.

Comparing these results with those of the full 12-spin calculation of the trimer plaquette, we observe that indeed all five different lowest eigenenergies can be identified (using their degeneracies and symmetries) with one of the five eigenenergies of the reduced four-spin model. We can thus directly infer from this comparison the effective coupling constants of the reduced model. In figure 9 we plot the effective low-energy parameters $j_1 - j_4$ as functions of the bare ones $(J, J_a, J_b)$, setting $J_a/J = 0.2$ and varying the ratio $J_b/J_a$. At the point $J_a = J_b$, and in fact in most of the parameter regime plotted, one observes a dominant nearest-neighbor exchange: however, the leading correction is $j_4$. Close to the transition from antiferromagnetic ($j_1 > 0$) to ferromagnetic ($j_1 < 0$) nearest-neighbor coupling, the diagonal four-spin exchange process $j_4$ becomes dominant but remains relatively small. While the effect of a $j_2$ and/or $j_3$ exchange has been well investigated in the literature (see, e.g., [15]), much less is known about the effect of $j_4$. Two-dimensional lattices of coupled trimers make it possible to realize exotic spin models and to probe the effect of diagonal four-spin exchange processes at low temperatures.

## 6. Discussion and summary

In the trinuclear copper complex $2b{\cdot}3CuCl_2{\cdot}2H_2O$, the single magnetic $Cu^{2+}$ trimers are connected via a strong network of O–H$\cdots$Cl hydrogen bonds to build up a layered quasi-2D system. The magnetic susceptibility and isothermal magnetization also clearly exhibit the low-dimensional magnetic character of this quantum spin system. Using a theoretical model of 2D coupled trimers, we extract the antiferromagnetic *intra*-trimer coupling constant $J/k_B = -15$ K and the *inter*-trimer coupling constants $J_{a,b}/k_B = -4$ K. For $Cu^{2+}$ ions linked pairwise by the carboxylate in a nearly planar quadratic coordination, this antiferromagnetic *intra*-trimer coupling constant appears surprisingly small. But, as seen in figure 1, the individual Cu coordination planes are tilted against each other so that a significant reduction of the magnetic coupling constant can be expected.

On the other hand, the antiferromagnetic *inter*-trimer couplings, which are mediated by the O–H$\cdots$Cl hydrogen bonds, have with $J_{a,b}/k_B = -4$ K an unexpected large value. But it is known from investigations performed on purely organic magnets that in these compounds hydrogen bonds not only link the individual spin carriers together to form a crystal lattice. These bonds are also responsible for the magnetic coupling with exchange constants of the order of a few kelvin [16, 17 and references therein].

Although both O–H$\cdots$Cl hydrogen bonds provide an antiferromagnetic exchange coupling between adjacent trimers, lowest-order perturbation theory shows that the resulting effective *inter*-dimer coupling $J_{eff}$ becomes ferromagnetic if $J_b < J_a/2$. Moreover, the application of the effective interacting-trimer model shows that, near the transition where the nearest-neighbor coupling changes sign, four-spin diagonal-exchange processes are dominant. It remains to be seen to what extent the ratio $J_b/J_a$ in $2b{\cdot}3CuCl_2{\cdot}2H_2O$ can be influenced by chemical substitution and/or hydrostatic pressure, making these interesting processes experimentally accessible.

With the trinuclear copper complex $2b{\cdot}3CuCl_2{\cdot}2H_2O$, we synthesized and investigated a low-dimensional quantum spin system which has an unusual magnetic topology. Furthermore, it is a compound which has the potential to be tuned either by chemical modification or external parameters such as hydrostatic pressure to a point where magnetic four-spin diagonal-exchange processes become relevant.

## Acknowledgment

Financial support by a SFB/TRR49 and by a DAAD/CAPES PROBRAL grant is acknowledged.

## References

[1] Schollwöck U, Richter J, Farnell D J and Bishop R F (ed) 2004 *Quantum Magnetism* (*Springer Lecture Notes in Physics*) (Berlin: Springer) doi:10.1007/696825
[2] de Jongh L J and Miedema A R 1972 *Adv. Phys.* **23** 1
[3] Miller J S and Drillon M (ed) 2001 *Magnetism: Molecules to Materials II* (New York: Wiley–VCH)
[4] Kahn O 1993 *Molecular Magnetism* (New York: VCH)
[5] Grigereit T E, Ramakrishna B L, Place H, Willett R D, Pellacani G C, Manfredini T, Menabue L, Bonamartini-Corradi A and Battaglia L P 1987 *Inorg. Chem.* **26** 2235–43
[6] Bond M R, Willett R D, Rubins R S, Zhou P, Zaspel C E, Hutton S L and Drumheller J E 1990 *Phys. Rev.* B **42** 10280–90
[7] Zaspel C E, Rubenacker G V, Hutton S L, Drumheller J E, Rubins R S, Willett R D and Bond M R 1988 *J. Appl. Phys.* **63** 3028–30
[8] Ferey G, Mellot-Draznieks C, Serre C, Millange F, Dutour J, Surblé S and Margiolaki I 2005 *Science* **309** 2040–2
[9] Chui S, Lo S, Charmant J, Orpen A and Williams I 1999 *Science* **283** 1148–50
[10] Livage C, Guillou N, Chaigneau J and Rabu P 2006 *Mater. Res. Bull.* **41** 981–6
[11] Wiehl L, Schreuer J, Haussühl E and Hofmann P 2009 *Z. Kristallogr. NCS* submitted

[12] Mukhopadhyay S, Mandal D, Chatterjee P B, Desplanches C, Sutter J P, Butcher R J and Chauhdury M 2004 *Inorg. Chem.* **43** 8501–9
[13] Pashchenko V, Brendel B, Wolf B, Lang M, Lyssenko K, Shchegolikhina O, Molodtsova Y, Zherlitsyna L, Auner N, Schütz F, Kollar M, Kopietz P and Harrison N 2005 *Eur. J. Inorg. Chem.* **23** 4617–25
[14] Schmidt H J and Kuramoto Y 1990 *Physica* C **167** 263–6
[15] Chubukov A, Gagliano E and Balseiro C 1992 *Phys. Rev.* B **45** 7889–98
[16] Romero F, Ziessel R, Bonnet M, Pontillou Y, Ressouche E, Schweizer J, Delley B, Grand A and Paulsen C 2000 *J. Am. Chem. Soc.* **122** 1298–309
[17] Rancurel C, Daro N, Borobia O B, Herdtweck E and Sutter J P 2003 *Eur. J. Org. Chem.* **1** 167–71